HHS Public Access

How to use fMRI functional localizers to improve EEG/MEG source estimation

Benoit R. Cottereau[a,b], **Justin M. Ales**[c], and **Anthony M. Norcia**[d]

[a]Université de Toulouse, Centre de Recherche Cerveau et Cognition, UPS, France

[b]CNRS UMR 5549, CerCo, Toulouse, France

[c]School of Psychology and Neuroscience | St Mary's Quad, South Street | University of St Andrews | St Andrews, KY16 9JP, UK

[d]Department of Psychology, Stanford University, Stanford, California

Abstract

EEG and MEG have excellent temporal resolution, but the estimation of the neural sources that generate the signals recorded by the sensors is a difficult, ill-posed problem. The high spatial resolution of functional MRI makes it an ideal tool to improve the localization of the EEG/MEG sources using data fusion. However, the combination of the two techniques remains challenging, as the neural generators of the EEG/MEG and BOLD signals might in some cases be very different. Here we describe a data fusion approach that was developed by our team over the last decade in which fMRI is used to provide source constraints that are based on functional areas defined individually for each subject. This mini-review describes the different steps that are necessary to perform source estimation using this approach. It also provides a list of pitfalls that should be avoided when doing fMRI-informed EEG/MEG source imaging. Finally, it describes the advantages of using a ROI-based approach for group-level analysis and for the study of sensory systems.

Keywords

EEG; fMRI; Source imaging; Data fusion; MEG

Introduction

The cortical generators of EEG/MEG measurements can be estimated by solving an inverse imaging problem where the unknown sources are distributed on an individual's cortex with their orientations fixed and orthogonal to the local surface (Dale and Sereno, 1993).

Corresponding Author: Benoit R Cottereau, **Address:** CNRS CERCO UMR 5549 Pavillon Baudot CHU Purpan BP 25202 31052 Toulouse Cedex, France, **Phone number:** + 33 (0)5-81-18-49-58, cottereau@cerco.ups-tlse.fr.

Typically, several thousand sources are needed to model the convolutions of the cortical manifold precisely, but only a hundred or so measurements are available. The associated inverse procedure is thus extremely ill-posed and has an infinity of solutions (Hämäläinen al., 1993). Conventional approaches to this issue introduce priors on the source distribution to constrain the estimation problem.

Over the two last decades, the emergence of functional imaging techniques, notably fMRI, has opened avenues to improve EEG/MEG source localization by fusing data acquired separately in the two modalities. Since the late 1990's, it has been proposed that the BOLD responses obtained from the same experiments could be introduced as prior in the source covariance matrix $\mathbf{R}$. For example, George et al., (1995) used BOLD activation maps to set the diagonal elements of $\mathbf{R}$ to non-zero values at source locations where the BOLD activations were above a given threshold. This approach makes the assumption that the generators of the BOLD responses are identical to those of the EEG/MEG measurements. While such a hypothesis might sometimes be partially true, there are also cases where the neural generators of the two signals are totally different (see e.g. Geukes et al., 2013). Several studies have proposed to address this issue by imposing a partial fMRI constraint (Ahlfors and Simpson, 2004; Dale et al., 2000; Liu et al., 1998, 2002) or by modeling more finely the relationship between the BOLD signals and the EEG/MEG measurements (Sato et al., 2004; Yoshioka et al., 2008; Liu and He, 2008; Ou et al., 2012). Although these approaches soften the impact of the discrepancies between the generators of the EEG/MEG and the BOLD, they do not fully eliminate them (Vanni et al., 2004). In addition, these approaches require that each EEG experiment has to be reproduced in fMRI, thereby increasing the acquisition time and costs associated with each study.

FMRI data can be used in a different way to serve as a source constraint. Rather than assuming correspondence between activation in replicated studies in EEG/MEG and fMRI, one can use fMRI to map out the structure of independent functional regions of interest. These regions of interest (ROIs) consist either of the topographic maps of the sensory surfaces onto cortex or cortical areas that are defined on the basis of their stimulus selectivity. Previous work has used the spatial correspondence between the stimulus space and brain regions, coupled with using multiple stimulus locations in EEG to constrain localization (Vanni et al., 2004; Di Russo et al., 2005; Hagler et al., 2009; Ales et al. 2010). Our work described here has developed an fMRI-informed EEG/MEG source imaging approach where the structure of the source correlation matrix is derived from a specific set of cortical regions that are determined once for any individual participant (Cottereau et al., 2012a). Mapping these regions provides several benefits. The regions of interest provide a basis for making not just an anatomically defined, but also a functionally defined cross-subject correspondence. The associated constraints are independent of any given experimental protocol and thus can be reused. Our approach is based on the biologically plausible assumption that the activity within an ROI is correlated. As the EEG/MEG signals are related to the neuron spiking rate (Hämäläinen et al., 1993; Logothetis, 2008) and the spiking rates of neurons within the same cortical area are correlated (Cohen and Maunsell, 2009; Kenet et al., 2003; Lampl et al., 1999), the voltages coming from nearby sources belonging to the same area should be highly similar. In addition to improving the spatial

resolution of the EEG/MEG reconstructions, this approach also leads to an ROI analysis that is based on functional correspondence. Functional ROI-based comparisons both simplify and increase the accuracy of the pooling of the results between subjects, because a co-registration of the individual anatomies, with its inevitable distortion is not necessary. Over the last several years, this approach has been used to study different properties of the visual system: motion processing (Cottereau et al., 2014a; Ales and Norcia, 2009), chromatic processing (Wang and Wade, 2011; Xiao and Wade, 2010), binocular disparity processing (Cottereau et al., 2011; 2012bc), attention (Kim and Verghese, 2012; Verghese et al., 2012; Palomares et al., 2012; Lauritzen et al., 2010), figure-ground segmentation (Appelbaum et al., 2006; 2008; 2010), perceptual decision-making (Cottereau et al., 2014b; Ales et al., 2013) and contrast normalization (Busse et al., 2009; Tsai et al., 2012). Beyond the scope of the visual system, this approach can easily be applied to other sensory systems where fMRI can be used to reliably map functional areas (see e.g. Barton et al., 2012 for the auditory system or Meier et al., 2013 for the sensory-motor system).

This mini-review is based on a talk that was given at the 'Cutting-EEG' workshop (Berlin, 2014). It describes the analysis pipeline and explains how to use functional areas defined from functional magnetic resonance imaging (fMRI) to inform the EEG/MEG inverse problem. It completes a recent publication (Cottereau et al., 2012a) that used simulations and real datasets to characterize the efficiency of the proposed method. In particular, it develops the advantages of using a ROI-based approach for group-level analysis.

Our goal is to explain the different steps that are necessary as well as the possible pitfalls that should be avoided when performing fMRI-informed EEG/MEG source imaging to the user who would be interested in using this approach. In the following, we first describe how to define the cortical source space (see the '*Source space definition*' section) and how to model the link between this source space and the EEG/MEG measurements (see '*Forward modeling of the cortical currents*' section). We then explain how to define functional areas using fMRI (see the '*Functional area definition using fMRI*' section) and how to introduce priors from these ROIs into the EEG/MEG source reconstruction problem (see the '*fMRI-informed inverse modeling of the cortical currents*' section'). Finally, we describe how to estimate the grouplevel cross-talk in a study (see the '*Cross-talk matrix*' section) and the possibilities that such an approach opens. For each of these steps, we briefly describe the aim and provide a detailed explanation of how this step was performed in our previous studies. We also discuss possible alternatives that might improve each step.

Material and method

Source space definition

Aim: In order to model the link between the EEG/MEG measurements and cortical activity, it is necessary to define a source space. Because the generators of the signals are believed to be mainly cortical, the source space is given by the cortical surface that is extracted from a structural scan of each subject.

How we currently do it: For tissue segmentation and registration with the functional scans, we collect a T1-weighted MRI data set at 3T. Our typical voxel acquisition resolution is 0.8

$\times\ 0.8 \times 0.8$ mm^3, which because of current software limits is resampled to $1 \times 1 \times 1$ mm^3. The FreeSurfer software package (http://surfer.nmr.mgh.harvard.edu) is used to extract both gray/white and gray/cerebrospinal fluid (CSF) boundaries. These surfaces can have different curvatures. In particular, the gray/white boundary has sharp gyri (the curvature changes rapidly) and smooth sulci (slowly changing surface curvature), while the gray/CSF boundary is the inverse, with smooth gyri and sharp sulci. To avoid these discontinuities, we generate a surface partway between these two boundaries that has gyri and sulci with approximately equal curvature. For each subject, the source space is given by his/her "midgray" cortical surface tessellation and consisted in 20,484 regularly spaced vertices (see figure 1-B). The distance between connected vertices is on average 3.7mm with standard deviation of 1.5 mm and range 0.1–11 mm. Current dipoles are placed at each of these vertices. Their orientations are constrained to be orthogonal to the cortical surface to diminish the number of parameters to be estimated in the inverse procedure (Hämäläinen et al., 1993).

Alternatives: Although we use FreeSurfer, several other packages can be used to extract the cortical surface from structural scans: e.g. the Anatomist software available in the BrainVISA environment (http://brainvisa.info) or BrainVoyager (http://www.brainvoyager.com, Goebel, 2012).

Forward modeling of the cortical currents

Aim: Model the relationship between the source space and the EEG/MEG measurements at the sensor level. For this step, it is necessary to take into account the different compartments within the head (CSF, skull and skin) (see e.g. Hallez et al, 2007). These compartments can be extracted from T1 and T2-weighted structural scanners of each individual subject. The source space also needs to be co-registered with the positions of the EEG electrodes.

How we currently do it: We collect a 3D T2-weighted data set at 3T. We typically acquire the T2-weighted scan in the same session as the T1 and use identical geometry. It is important for the scan parameters of the T2 acquisition to be chosen in such a way as to reduce signal from spongy bone in the skull. Our typical voxel resolution is $0.8 \times 0.8 \times 0.8$ mm^3. The FSL toolbox (http://www.fmrib.ox.ac.uk/fsl/) is used to segment from the individual T1- and T2-weighted MRI scans contiguous volume regions for the inner skull, outer skull, and scalp. These MRI volumes are then converted into inner skull, outer skull, and scalp surfaces (Smith 2002; Smith et al., 2004) that defined the boundaries between the brain/CSF and the skull, the skull and the scalp, and the scalp and the air (see figure 1-B). Following each EEG recording session, a Polhemus FASTRAK system is used to record the electrode positions, fiducial landmarks (nasion, left, and right tragus), and several tens of points distributed around the scalp and face surface. Co-registration of the electrode positions to the MRI head surface is performed using a least squares fitting routine in MATLAB. The algorithm starts by first using the three digitized fiducial landmarks along with their visible locations on the anatomical MRI to perform an initial alignment to the MRI coordinate frame. From this initial estimate, we find the rigid body transform that minimizes a cost function that combines the distance from digitized scalp points and the digitized electrode positions. This approach provides an accurate co-registration whose mislocalization error typically ranges below 3 mm. The source space, the 3D electrode

locations, and the individually defined boundaries are then combined with the MNE software package (http://www.nmr.mgh.harvard.edu/martinos/userInfo/data/sofMNE.php) to characterize the electric field propagation with a three-compartment boundary element method (BEM) (Hämäläinen and Sarvas, 1989). The resulting forward model is linear and links the activity of the 20,484 cortical sources to the voltages recorded by the sensors. Mathematically, this forward model can be written as:

$$\mathbf{M}(t) = \mathbf{G}\mathbf{J}(t) + \varepsilon(t),$$

where $\mathbf{M}$ is a column vector containing the m measurements on the EEG/MEG sensor array at instant t; $\mathbf{J}$ is a column vector of the n unknown source amplitudes of all elementary sources in the model with zero mean and a covariance matrix $\mathbf{R}$ (size n * n); $\mathbf{G}$ (size m * n) is the forward gain matrix sampled at the sensor array and ε (size m * 1) is an additive nuisance term with zero mean and a covariance matrix $\mathbf{C}$ (size m * m).

Alternatives: Although we use the MNE software to generate our forward model, several other options exist. Boundary element models for EEG are also available in Brainstorm (Tadel et al., 2011), FieldTrip (Oostenveld et al., 2011) or SPM8 (Litvak et al., 2011).

In our studies, the source orientation is constrained to be normal to the cortical surface. Other studies chose to use a *loose* constraint where three orientation parameters are estimated for each source (Uutela et al., 1999; Lin et al., 2006). Lin et al. (2006), showed that applying a loose-orientation constraint to a relatively coarse model of about 7,500 dipolar sources improved the localization performances of a variety of distributed source imaging approaches by a few millimeters with respect to image models with strict or totally free orientations. The implementation of a loose-orientation version of our approach is straightforward.

BEM methods assume homogeneity and isotropy within each region of the head. It ignores anisotropy in white matter tracts in the brain in which conduction is more important along the axonal fibers compared to the transverse direction (see e.g. Wolters et al., 2006). Similarly, the sinuses and diploic spaces in the skull make it very inhomogeneous. To take into account these different factors, it is possible to compute the forward model from finite element methods (FEM). These methods can, for example, use diffusion tensor imaging (DTI) to accurately model the anisotropy within the white matter. They might therefore improve the forward model and the accuracy of the associated inverse (Gullmar et al., 2010). Note that all the inverse techniques described in this mini review could be directly applied to a forward model obtained from a finite element method.

Functional area definition using fMRI

Aim: localize the different functional areas using fMRI that will be used to constrain the inverse procedure.

How we currently do it: For functional MRI (fMRI), we employ a single-shot, gradient-echo planar imaging (EPI) sequence (TR/TE = 2,000/28 ms, flip angle 80, 126 volumes per run) with a typical voxel size of $1.7 \times 1.7 \times 2$ mm^3 (128×128 acquisition matrix, 220-mm field

of view, bandwidth 1,860 Hz/pixel, echo spacing 0.71 ms). We acquire 30 slices without gaps, positioned approximately parallel to the parietal occipital sulcus. Once per session, a 2D SE T1-weighted volume is acquired with the same slice specifications as the functional series in order to facilitate registration of the fMRI data to the anatomical scan. The general procedures for these scans (head stabilization, visual display system, etc.) are standard and have been described in detail elsewhere (Brewer et al., 2005).

Retinotopic field mapping using rotating wedges and expanding/contracting rings (cycles of 12 TRs) produce ROIs corresponding to visual cortical areas V1, V2v, V2d, V3v, V3d, V3A, and V4 in each hemisphere (Tootell and Hadjikhani, 2004). These stimuli are shown in figure 2 and their complete description can be found in (Brewer et al., 2005). For each subject, the retinotopic maps are acquired during one session that lasts less than an hour. We record 4 runs of wedges and 4 runs of rings. Each run contains 126 volumes (4min12s). We discard the 6 first volumes from the analysis to allow for both the magnetization history and visual stimulation response to reach steady-state. The remaining 120 cycles contains exactly 10 cycles of our stimuli and are analyzed in the Fourier domain. For each voxel, its preferred polar angle (for the wedge stimuli) and eccentricity (for the ring stimuli) in the visual field are given by the phase of the Fourier coefficients at the stimulation frequency. The retinotopic ROIs are then manually defined using these values.

ROIs corresponding to hMT+ are identified with low-contrast motion stimuli similar to those described in (Huk and Heeger 2002). The LOC is defined with a block-design fMRI localizer scan. During this scan, the observers view blocks of images depicting common objects (12 s/block) alternating with blocks containing scrambled versions of the same objects. The stimuli are those used in a previous study (Kourtzi and Kanwisher, 2002). The regions activated by these scans include an area lying between the V1/V2/V3 foveal confluence and hMT+ that we identify as LOC. This definition covers almost all regions (e.g., V4d, LOC, LOp) that have previously been identified as lying within object-responsive lateral occipital cortex (Kourtzi and Kanwisher, 2002). The LOC and hMT+ localizers are recorded during one session that lasts less than one hour and contains 4 runs (126 volumes) for each localizer.

Our data are first corrected for gradient non-linearity distortion (see e.g. Jovicich et al., 2006) using tools provided by our MRI manufacturer. Slice-timing correction and motion correction are then performed using the FSL toolbox. For motion correction, we use the mcflirt tool (see Jenkinson et al., 2002). Our analysis of the fMRI data is finally done using the VISTA software (http://white.stanford.edu/software/) or the AFNI package.

These different functional localizers and the associated ROIs from a typical subject are shown in Figure 2-A. All these fMRI analyses were performed using the Vista software.

Alternatives: Atlas-fitting algorithms (see e.g. Dougherty et al., 2003, Hagler & Dale, 2013) can be used to automatically extract the retinotopic ROIs from BOLD responses to rotating wedges and expanding/contracting rings). This approach should permit a more accurate definition of the retinotopic ROIs. Recent studies have also shown that it is possible to define retinotopic maps on the ventral pathway: VO-1 and V0-2 (Brewer et al., 2005) and at

the level of the lateral occipital cortex (Larson and Heeger, 2006). Manipulating attention, it is possible to define additional retinotopic maps in the parietal cortex (Silver et al., 2005; Swisher et al., 2007; Silver and Kastner). Studies on the visual system have recently described various additional localizers that could easily be introduced in our approach: FFA (Kanwisher et al., 1997), PPA (Aguirre et al., 1998), V6 (Cardin et al., 2012), CSv (Wall and Smith, 2008; Pitzalis et al., 2013), KO (Tyler et al., 2006) (see figure 2-B). Functional localizers in other sensory modalities have also recently been proposed in the auditory domain (tonotopic maps, Barton et al., 2012) and in the sensory-motor system (Meier et al., 2013). Some ROIs, such as hMT+ contain multiple, distinct visual areas, that could potentially have different activation time courses or response properties. In order to model more finely the intra-area correlation, our approach could take into account these different sub-divisions. For example in the case of hMT+, motion-based fMRI localizers permit a differentiation between MT and MST (Dukelow et al., 2001; Huk et al., 2002). Even finer subdivisions of this part of the cortex can be obtained from retinotopic mapping (Kolster et al., 2010). Recent studies suggested that it is possible to extract the early visual areas from their anatomical and/or geometrical properties (Glasser & Van Essen, 2011; Benson et al., 2012; Bridge et al., 2013; Benson et al., 2014, see the FreeSurfer package for an atlas-based definitions of V1, V2 and hMT+). If these results can be confirmed and extended to higher-level visual areas, they open the exciting possibility to apply our approach without the need to record additional fMRI data.

EPI can sometimes suffer from intensity distortion caused by the B_0 field inhomogeneity induced by magnetic susceptibility variations. Methods have been proposed to remove these distortions (see e.g. Holland et al., 2010). The application of these methods in our pipeline would probably improve the quality of the data.

fMRI-informed inverse modeling of the cortical currents

Aim: use the functional localizers to constrain the estimation of the cortical activity generating the EEG/MEG measurements and characterize the activity within the ROIs

How we currently do it: A classical solution to the forward model (see the '*Forward modeling of the cortical currents*' section above) is to use an L2 regularized minimum-norm inverse (Hämäläinen et al., 1993). In this case, the solution has a closed form and can be written:

$$\hat{J} = RG'\left(GRG' + \lambda^2 C\right)^{-1} M$$

where λ is a regularization parameter. In absence of any prior on the source distribution, the source covariance matrix **R** is often equal to the identity matrix. In our case, we introduce our knowledge of the functionally defined ROIs into this matrix. Our aim is to decrease the tendency of the minimum-norm procedure to smooth activity over very large surfaces and across different functional areas. In order to do so, we enforce a local correlation constraint within each area using the first- and second- order neighbors on the cortical tessellation with a weighting function equal to 0.5 for the first order and 0.25 for the second (i.e. the off-diagonal elements of **R** corresponding to neighbor sources belonging to the same functional

ROI are increased, see figure 2-C). This modification of the correlation matrix **R** therefore respects both retinotopy and areal boundaries and permits us to dissociate the signals from different areas, unlike other smoothing methods such as LORETA that apply the same smoothing rule throughout cortex (Pascual-Marqui et al., 1994). In practice, the full correlation matrix **R** can be very large when considering a realistic representation of the cortical surface (i.e. we saw in the '*Source space definition*' section that about 20,000 sources are necessary). However, as our model does not consider the inter-area correlations, only the sub-parts of **R** that correspond to the functional areas are modified (see figure 2C). **R** is therefore sparse and can be stored easily. Our inverse solution involves a Cholesky decomposition of **R** and consequently of each of the sub-parts of **R** associated with a functional area. For some of these areas, modifying the off-diagonal elements of the corresponding sub-part of **R** may lead to non semi-definite matrices. In this case, we can rewrite the concerned sub-parts from its eigenvalue decomposition by setting all the negative eigenvalues to 10e-5. This leads to a decomposable matrix **R** whose global correlation properties remain unchanged. Note that because **R** is a block-diagonal matrix, this operation is equivalent to setting all the negative eigenvalues of **R** to 10e-5.

Several options are possible for the choice of the regularization parameter λ. It can be determined from an eigenvalue decomposition of the forward matrix **G** or directly estimated from the data. In our case, we use a generalized cross-validation approach. This technique uses a leave-one-out procedure to robustly estimate the noise in the measurements and computes the value of λ that minimizes it (Reeves, 1994). It has been adopted in a number of estimation problems, including EEG (Babiloni et al., 2004) but also MEG (Cottereau et al., 2007) brain imaging. For this computation, we use Matlab routines that were previously described in (Hansen, 1994). Once the current density is obtained for each cortical source, ROI-level responses can be computed by averaging the time courses from all the sources within each ROI. We refer to the combination of L2 inversion constrained by functional areas as the Functional Area Constrained Estimator (FACE) (Cottereau et al., 2012a). For many ROI's, especially large ones, opposite polarity dipoles can be present within the ROI. When the time courses from these sources are averaged, they will cancel each other. However, when the whole or majority of an ROI is activated, any cancellation of the measured response should be similar to the cancelation that occurs in the measured response to an extended patch of cortex (Ahlfors et al., 2010). Making mistakes because of confusing activation *between* ROI's is a more important problem than getting the absolute magnitude of activation *within* an ROI correct. To this end we feel that the crosstalk matrix for the different ROI's (see the next section) provides the best quantification of whether opposite polarity sources are a problem. Cancellation effects are nonetheless an inherent problem with any form of EEG recording, and their possible presence should always be born in mind.

Alternative: in our studies, we introduced our prior on the source correlation within a classical L2 minimum-norm estimator. We have shown however that this prior can be successfully introduced within different inverse approaches (see Cottereau et al., 2012a) like LORETA (Pascual-Marqui et al., 1994) or MSP (Mattout et al., 2006). In the recent years, L1 approaches have been described in the literature (Uutela et al., 1999; Ding & He, 2008). They could be directly used here. The values of the off-diagonal elements of **R** are fixed in

the current version of our approach. Recent techniques based on Bayesian inference could be used to estimate these values from the data (see e.g. Daunizeau et al., 2005 or Henson et al., 2010).

Misalignment of the EEG/MEG and MRI coordinate frames or errors in constructing a cortical surface can lead to inaccuracies in the dipole orientation used in the forward model. To diminish the impact of these errors on source reconstruction, we saw in the '*Forward modeling of the cortical currents*' section that several approaches proposed to use a loose constraint on dipole orientation (see Uutela et al., 1999 or Lin et al., 2006). The combination of these approaches with FACE is straightforward.

The cross-talk matrix: an efficient way to characterize the accuracy of a ROI-based EEG/MEG analysis

Aim: characterize the reliability of an inverse.

The researcher who wants to use source imaging should always be aware of the limited accuracy of an inverse solution when analyzing data and interpreting results. This can be done through numerical simulations where the cortical activity is known (see e.g. Cottereau et al., 2012a). In particular, the accuracy of a ROI-based approach can be characterized from a cross-talk matrix. Cross-talk refers to the neural activity generated in other ROIs that is attributed to a particular ROI, due to the smoothing of the electric field by the head volume.

How we currently do it: for each subject, we simulate the cross-talk by placing sources in one ROI and estimating their contribution to other ROIs, using the same forward and inverse methods described above. The global cross talk matrix (i.e., averaged across all the subjects who participated in our EEG experiment) is shown in figure 3-A for seven ROIs (V1, V2, V3, V4, LOC, V3A, and hMT+); the cross talk magnitude shown in the matrix is proportional to activity originating in the ROI where the cross talk is being estimated. This cross-talk matrix was obtained using an inter-ROI correlation prior. To illustrate that this prior diminishes cross-talk error, we show the cross-talk matrices with and without a FACE prior in supplementary figure 1.

The crosstalk matrix (figure 3-A) indicates that large areas (e.g. V1) or areas with high curvature (e.g. hMT+) do not necessarily have the worst crosstalk and therefore that their estimated time-courses is not too much affected by opposite polarity sources (see the previous section). A very important point about functional areas is that their shape, size and position on the cortical mantel varies significantly across subjects. For example, Dougherty et al., (2003) showed that the surface of the early visual areas V1, V2 and V3 can vary by as much as a factor of three between subjects. Substantial variability also exists in their shape and therefore in the orientation of these retinotopic areas. Important inter-subject variability has also been described for higher-level visual areas (Duncan et al., 2009). Because of this variability, the cross-talk from one ROI to the others varies considerably across subjects. This property is illustrated in figure 3-B where the visual areas and associated cross-talk matrices are shown for 4 different subjects. For group-level studies, this variability is actually a strength because the cross-talk into a target areas tends to cancel across subjects. To illustrate this property, we can compute a cross-talk error for an increasing number of

subjects. This error is given by the norm of the difference between the identity matrix and the average cross-talk matrix. It is equal to zero when there is no cross-talk. To facilitate visualization, this error was normalized by its value for one unique subject. The results obtained for up to 11 subjects are shown in figure 3-C. For more than 6 subjects, this error is a factor of two less than that for a single-subject inverse.

What can be done with a ROI-based analysis?

ROI-based analysis has several advantages over the whole-brain analysis that is more classically used in EEG/MEG imaging studies. First, it allows a direct comparison of activations between functionally equivalent sources across subjects. Given ROI definitions, it is not necessary to first co-register the subject's brain to an anatomical common space. The method therefore avoids all the issues associated with these co-registrations. The method also allows one to compare EEG/MEG results to those obtained from other studies using other methods, such as fMRI or single-unit physiology where the same ROIs were defined. Finally, it greatly simplifies the multiple comparison problem in statistics, as the number of ROIs is 2 orders of magnitude smaller that the number of cortical sources.

Over the last years, the ROI-based approach described in this review has been used to characterize the dynamics and more recently the functional connectivity (Cottereau et al., 2014a) of the responses within the different visual areas. As an example, figure 4 shows the results obtained in one of our previous EEG studies where we were interested in the cortical mechanisms implied in decision-making (Cottereau et al., 2014b).

In this example, subjects had to detect a horizontal disparity (i.e. a depth) increment within a temporal sequence where a disc appeared and disappeared at 1 Hertz (see figure 4A). Subjects signaled their detection by pressing a button on the keyboard. Our ROI-based analysis revealed that the dynamics of the responses were very different in the different ROIs. We show here the responses for the hits vs misses (i.e. the evoked potentials corresponding to the trials where the target was detected vs missed) in 3 representative ROIs: V1, V3A and V4. This comparison is shown for stimulus-locked (figure 4C) and response-locked (figure 4D) data. The complete details of the analysis and the responses in the other ROIs can be found in (Cottereau et al., 2014b). What is interesting to observe is how different the shapes of the responses in the three ROIs are. While responses for Hits and Misses in V1 are very similar, significant differences appear first in the V4 and then in the V3A ROIs. This illustrates well how our ROI-based approach can dissociate the responses from the different functional ROIs. We noted above that defining ROIs facilitates the comparison with results obtained in other studies. In this particular case, we have noted that other imaging data in human (Neri et al., 2004) and electrophysiological recordings in macaque (Shiozaki et al., 2012) have also implicated V4 in depth encoding and discrimination. Using a very similar paradigm and the same approach, we investigated the neural mechanisms involved in shape discrimination (see Ales et al., 2013). In this case, the first ROI that showed a significant decision-related activity was the LOC ROI, extending our knowledge of decision networks in human cortex both in terms of cortical organization, but also in terms of the temporal evolution of response over the different areas comprising the underlying perceptual, decision, and motor response networks..

Discussion

Here we have described an approach to multi-modal data fusion that uses functionally defined ROIs to constrain the solution of EEG/MEG imaging problems. We have focused on EEG recording examples, but the same methodology can be directly applied to MEG recordings. Our method allows for the introduction of a prior on the covariance matrix of the current source distribution in the inverse procedure. This prior is quite detailed and is based on biologically plausible assumptions about the existence of correlations between neighboring sources embedded in the same topographically organized functional area (see e.g. Cohen and Maunsell, 2009). We have previously documented the improvements brought by such priors using Monte-Carlo simulations (Cottereau et al., 2012a). We have used this approach to study the visual system, but our method can be directly applied to other sensory modalities that have multiple topographically organized maps, e.g. in the auditory (Barton et al., 2012) or sensory-motor (Meier et al., 2013) systems. The search for a better parcellation of cortex into functional areas is being advanced both through the use of fMRI but also anatomical properties extracted from structural images (Glasser & Van Essen, 2011; Benson et al., 2012; Bridge et al., 2013; Benson et al., 2014). Cortical parcellation is currently an active field of research and we anticipate that more and more precise functional cartographies of the human brain will emerge soon and that these new parcellation schemes can be used to good effect with our approach. Moreover, functionally defined ROI's are likely to be connected by specific white matter tracts. Many cortical tracts can now be identified automatically using Diffusion Tensor Imaging (Yeatman et al., 2012) and it may be possible to use this connectivity information to further tailor the source-covariance matrix on the assumption that areas that are anatomically connected are likely to also have functionally correlated activity. As we have noted, the use of individually defined ROI's for group-level analysis allows us to improve the spatial resolution of EEG or MEG-based imaging beyond what can be achieved at the single subject level. On a practical level, because the ROIs are not defined using a parallel fMRI study with similar stimuli, the inverse can be defined once for a given participant and reused for a wide range of experiments. Finally, an ability to meaningfully relate EEG/MEG activity to identified cortical areas facilitates the comparison of these results with those obtained by other methods that also acquire data from identified cortical regions (e.g. fMRI and single-unit physiology).

We have described here the different steps that are necessary to reproduce our technique. In particular, we provided a detailed list of the software that we are currently using in our analysis pipeline. As we have seen, other alternatives exist that should lead to qualitatively similar results. We also suggested that recent developments in forward modeling (see the '*Forward modeling of the cortical currents*' section) could probably improve our analysis pipeline (e.g. by using more realistic forward models). In all our studies, we used an L2 minimum-norm procedure. Our choice was mainly motivated by the fact that this method is well understood, easy to compute and is widely used in the neuroscience community as emphasized by the increasing number of associated articles published in the last years (see e.g. Florin et al., 2013; Khan et al., 2013; Park et al., 2014). However, our priors can be directly introduced into other reconstruction techniques if they include the covariance matrix

of the cortical current distributions **R** in their inverse procedure. For example, we recently evaluated the performance of our approach using two other standard source estimators (i.e., a LORETA inverse and a Multiple Sparse Prior (MSP) inverse) and demonstrated that our method provided enhanced source estimation for both of them (Cottereau et al., 2012a). We anticipate that algorithms based on L1 (Ding & He, 2008) or other norms (Auranen et al., 2005) will also benefit from these types of prior.

Other fMRI-informed EEG source imaging approaches

We have discussed in the introduction methods originally introduced by Dale and Sereno (1993) that use the fMRI data to constrain/inform the EEG/MEG source localization problem. These approaches make the assumption that the cortical origins of the BOLD and EEG/MEG signals measured from the same stimuli are identical. However, this is only sometimes the case (see e.g. Geukes et al., 2013). Recent reconstruction algorithms have dealt with this issue by modeling more finely the relationship between the BOLD signals and the EEG/MEG measurements. For example, Sato et al. (2004) used a Bayesian approach where the fMRI information is imposed as a prior on the variance of the source distribution rather than on the variance itself. This choice softens the errors caused by the discrepancies between the BOLD and EEG/MEG signals. The efficiency of this method was recently demonstrated on data acquired during the stimulation of different part of the visual field (Yoshioka et al., 2009). In Henson et al., (2010), each fMRI cluster is treated as an independent prior whose pertinence for source reconstruction is evaluated using a parametric empirical Bayesian framework. In Ou et al., (2010), the source weights are evaluated from both the fMRI and EEG/MEG data using a re-weighted minimum-norm algorithm. While these different techniques have proven to be accurate on both synthetic and real data, their use is nonetheless complicated at the scale of group studies, as they require a new fMRI acquisition every time a change is introduced in the stimulus. It is however interesting to note that our prior on intra-ROI correlation could easily be introduced within Bayesian model selection techniques such as the one described in Henson et al. (2010) (see also Daunizeau et al., 2005). In this context, Bayesian inference could characterize the relevance of our model and possibly determine the optimal values to be used in the off-diagonal elements of **R**.

Prior research has also taken another strategy – using the fine spatial organization of an area to help constrain localization results (Vanni et al., 2004; Hagler et al., 2009; Ales et al., 2010). These methods use fMRI to map the topographic correspondence of a cortical region with the stimulus space (usually the visual field, but it could be any known topographic map). Several stimuli that differ just in their location in the stimulus space along with their known cortical projection are then used in the source localization step. The algorithms used to enforce the fMRI based-constraints have taken several forms. Vanni et al. (2004) used the topographic locations to seed that starting locations of dipoles (see also Pitzalis et al., 2012). Responses from several stimulus locations were then compared. Response components that were consistent across the locations were taken as the correct solution. The method can be taken a bit further if one can assume that the neural response properties do not vary quickly within a topographically mapped region. This is similar to the assumption used in the FACE method described above where activity is constrained to vary smoothly within, but not

between ROI's. If activity in a topographically mapped ROI is relatively homogeneous, then changing the location of a stimulus does not dramatically change the neural response. Using this assumption, if one uses the same stimulus at multiple locations, one can constrain the recovered activity to be similar across presented locations. Slotnick et al. (1999) and Hagler et al. (2009) used the assumption that it is possible to distinguish between activation in neighboring, very closely spaced ROI's (e.g. V1 vs V2). All of these methods also have the advantage of being able re-use the fMRI-acquired dataset because a participant's topographic map in cortex does not vary. Therefore, these methods can then be used in the analysis of a variety of stimuli.

Conclusion

This mini-review describes a cutting-edge EEG/MEG technique that uses functional ROIs defined by fMRI to constrain the source localization problem. This technique has been used to study the visual system but can easily be extended to other sensory and cognitive systems. We describe here our analysis pipeline in detail and suggest several directions that future studies could take to improve even further the current spatial resolution of the approach. We also demonstrate the advantages of using this ROI-based approach for neuroscience studies, specifically in the case of group-level analysis.

Supplementary Material

Refer to Web version on PubMed Central for supplementary material.

Acknowledgments

Bibliography

Aguirre GK, Zarahn E, D'Esposito M. An area within human ventral cortex sensitive to "building" stimuli: evidence and implications. Neuron. 1998; 21:373–383. [PubMed: 9728918]

Ales J, Carney T, Klein SA. The folding fingerprint of visual cortex reveals the timing of human V1 and V2. Neuroimage. 2010; 49:2494–2502. [PubMed: 19778621]

Ales JM, Appelbaum LG, Cottereau BR, Norcia AM. The time course of shape discrimination in the human brain. NeuroImage. 2013; 67:77–88. [PubMed: 23116814]

Ahlfors SP, Han J, Lin FH, Witzel T, Belliveau JW, Hämäläinen MS, Halgren E. Cancellation of EEG and MEG signals generated by extended and distributed sources. Human brain mapping. 2010; 31(1):140–149. [PubMed: 19639553]

Appelbaum LG, Wade AR, Vildavski VY, Pettet MW, Norcia AM. Cue invariant networks for figure and background processing in human visual cortex. J Neurosci. 2006; 26:11695–11708. [PubMed: 17093091]

Auranen T, Nummenmaa A, Hämäläinen MS, Jääskeläinen IP, Lampinen J, Vehtari A, Sams M. Bayesian analysis of the neuromagnetic inverse problem with Lp-norm priors. NeuroImage. 2005; 26(3):870–884. [PubMed: 15955497]

Babiloni F, Babiloni C, Carducci F, Romani GL, Rossini PM, Angelone LM, Cincotti F. Multimodal integration of EEG an MEG data: A simulation study with variable signal-to-noise ratio and number of sensors. Hum Brain Mapp. 2004; 22:52–62. [PubMed: 15083526]

Baillet SM, Mosher JC, Leahy RM. Electromagnetic brain mapping. IEEE Signal Process Mag. 2001; 18:14–30.

Barton B, Venezia JH, Saberi K, Hickok G, Brewer AA. Orthogonal acoustic dimensions define auditory field maps in human cortex. Proc. Natl. Acad. Sci. U.S.A. 2012; 109:20738–20743. [PubMed: 23188798]

Benson NC, Butt OH, Datta R, Radoeva PD, Brainard DH, Aguirre GK. The retinotopic organization of striate cortex is well predicted by surface topology. Curr Biol. 2012; 22:2081–2085. [PubMed: 23041195]

Benson NC, Butt OH, Brainard DH, Aguirre GK. Correction of Distortion in Flattened Representations of the Cortical Surface Allows Prediction of V1–V3 Functional Organization from Anatomy. PLoS computational biology. 2014; 10(3):e1003538. [PubMed: 24676149]

Brewer AA, Liu J, Wade AR, Wandell BA. Visual fields maps and stimulus selectivity in human ventral occipital cortex. Nature Neuroscience. 2005; 8:1102–1109.

Bridge H, Clare S, Krug K. Delineating extrastriate visual area MT (V5) using cortical myeloarchitecture. NeuroImage. 2013; 93(2):231–236. [PubMed: 23541801]

Busse L, Wade AR, Carandini M. Representation of concurrent stimuli by population activity in visual cortex. Neuron. 2009; 64(6):931–942. [PubMed: 20064398]

Cardin V, Sherrington R, Hemsworth L, Smith AT. Human V6: functional characterization and localization. PLoS ONE. 2012; 7:e47685. [PubMed: 23112833]

Cohen MR, Maunsell JH. Attention improves performance primarily by reducing interneuronal correlations. Nat Neurosci. 2009; 12:1594–1600. [PubMed: 19915566]

Cottereau B, Jerbi K, Baillet S. Multiresolution imaging of MEG cortical sources using an explicit piecewise model. Neuroimage. 2007; 38:439–451. [PubMed: 17889564]

Cottereau BR, McKee SP, Ales JM, Norcia AM. Disparity tuning of the population responses in the human visual cortex: an EEG source imaging study. J Neurosci. 2011a; 31(3):954–965. [PubMed: 21248120]

Cottereau B, Lorenceau J, Gramfort A, Clerc M, Thirion B, Baillet S. Phase Delays within Visual Cortex Shape the Response to Steady-State Visual Stimulation. NeuroImage. 2011b; 54(3):1919–1929. [PubMed: 20937397]

Cottereau BR, Ales JM, Norcia AM. Increasing the Accuracy of Electromagnetic Inverses Using Functional Area Source Correlation Constraints. Human Brain Mapping. 2012a; 33(11):2694–2713. [PubMed: 21938755]

Cottereau BR, McKee SP, Ales JM, Norcia AM. Disparity-specific spatial interactions: Evidence from EEG source imaging. J Neurosci. 2012b; 32(3):826–840. [PubMed: 22262881]

Cottereau BR, McKee SP, Norcia AM. Bridging the gap: global disparity processing in the human visual cortex. J Neurophysiol. 2012c; 107:2421–2429. [PubMed: 22323636]

Cottereau BR, McKee SP, Norcia AM. Dynamics and cortical distribution of neural responses to 2D and 3D motion in human. J Neurophysiol. 2014a; 111:533–543. [PubMed: 24198326]

Cottereau BR, Ales JM, Norcia AM. The evolution of a disparity decision in human visual cortex. NeuroImage. 2014b; 92:193–206. [PubMed: 24513152]

Dale A, Sereno M. Improved localization of cortical activity by combining EEG and MEG with MRI surface reconstruction: A linear approach. J. Cogn. Neurosci. 1993; 5:162–176. [PubMed: 23972151]

Daunizeau J, Grova C, Mattout J, Marrelec G, Clonda D, Goulard B, Benali H. Assessing the relevance of fMRI-based prior in the EEG inverse problem: a Bayesian model comparison approach. IEEE Transactions on Signal Processing. 2005; 53(9):3461–3472.

Ding L, He B. Sparse source imaging in electroencephalography with accurate field modeling. Hum Brain Mapp. 2008; 29:1053–1067. [PubMed: 17894400]

Di Russo F, Pitzalis S, Spitoni G, Aprile T, Patria F, Spinelli D, Hillyard SA. Identification of the neural sources of the pattern-reversal VEP. Neuroimage. 2005; 24(3):874–886. [PubMed: 15652322]

Dougherty RF, Koch VM, Brewer AA, Fischer B, Modersitzki J, Wandell BA. Visual field representations and locations of visual areas V1/2/3 in human visual cortex. J Vision. 2003; 3:586–598.

Dukelow SP, DeSouza JF, Culham JC, van den Berg AV, Menon RS, Vilis T. Distinguishing subregions of the human MT+ complex using visual fields and pursuit eye movements. Journal of Neurophysiology. 2001; 86(4):1991–2000. [PubMed: 11600656]

Duncan KJ, Pattamadilok C, Knierim I, Devlin JT. Consistency and variability in functional localisers. Neuroimage. 2009; 46:1018–1026. [PubMed: 19289173]

Florin E, Bock E, Baillet S. Targeted reinforcement of neural oscillatory activity with real-time neuroimaging feedback. NeuroImage. 2013; 88C:54–60. [PubMed: 24211817]

George J, Mosher J, Schmidt D, Aine C, Wood C, Lewine J, Sanders J, Belliveau J. Functional Neuroimaging by Combined MRI, MEG and fMRI. Hum Brain Mapp. 1995; S1:89.

Glasser MF, Van Essen DC. Mapping human cortical areas in vivo based on myelin content as revealed by t1- and t2-weighted MRI. J Neurosci. 2011; 31:11597–11616. [PubMed: 21832190]

Goebel R. BrainVoyager – past, present, future. Neuroimage. 2012; 62:748–756. [PubMed: 22289803]

Gullmar D, Haueisen J, Reichenbach JR. Influence of anisotropic electrical conductivity in white matter tissue on the EEG/MEG forward and inverse solution. a high-resolution whole head simulation study. Neuroimage. 2010; 51:145–163. [PubMed: 20156576]

Hagler DJ, Halgren E, Martinez A, Huang M, Hillyard SA, Dale AM. Source estimates for MEG/EEG visual evoked responses constrained by multiple, retinotopically-mapped stimulus locations. Human Brain Mapping. 2009; 30(4):1290–1309. [PubMed: 18570197]

Hagler DJ, Dale AM. Improved method for retinotopy constrained source estimation of visual-evoked responses. Human brain mapping. 2013; 34(3):665–683. [PubMed: 22102418]

Hallez H, Vanrumste B, Grech R, Muscat J, De Clercq W, Vergult A, D'Asseler Y, Camilleri KP, Fabri SG, Van Huffel S, Lemahieu I. Review on solving the forward problem in EEG source analysis. Journal of NeuroEngineering and Rehabilitation. 2007; 4(46)

Hämäläinen MS, Sarvas J. Realistic conductivity geometry model of the human head for interpretation of neuromagnetic data. IEEE Trans Biomed Eng. 1989; 36:165–171. [PubMed: 2917762]

Hämäläinen M, Hari R, Ilmoniemi R, Knuutila J, Lounasmaa O. Magnetoencephalography: theory, instrumentation and applications to the non invasive study of human brain function. Rev. Mod. Phys. 1993; 65:413–497.

Hansen P. Regularization tools: a Matlab package for analysis and solution of discrete ill-posed problems. Numerical Algorithms. 1994; 6:1–35.

Henson RN, Flandin G, Friston KJ, Mattout J. A Parametric Empirical Bayesian framework for fMRI-constrained MEG/EEG source reconstruction. Human brain mapping. 2010; 31(10):1512–1531. [PubMed: 20091791]

Holland D, Kuperman JM, Dale AM. Efficient correction of inhomogeneous static magnetic field-induced distortion in Echo Planar Imaging. Neuroimage. 2010; 50(1):175–183. [PubMed: 19944768]

Huk AC, Heeger DJ. Pattern-motion responses in human visual cortex. Nat Neurosci. 2002; 5:72–75. [PubMed: 11731801]

Huk AC, Dougherty RF, Heeger DJ. Retinotopy and functional subdivision of human areas MT and MST. The Journal of Neuroscience. 2002; 22(16):7195–7205. [PubMed: 12177214]

Im CH, Gururajan A, Zhang N, Chen W, He B. Spatial resolution of EEG cortical source imaging revealed by localization of retinotopic organization in human primary visual cortex. J Neurosci Methods. 2007; 161:142–154. [PubMed: 17098289]

Jenkinson M, Bannister P, Brady JM, Smith SM. Improved Optimisation for the Robust and Accurate Linear Registration and Motion Correction of Brain Images. NeuroImage. 2002; 17(2):825–841. [PubMed: 12377157]

Jovicich J, Czanner S, Greve D, Haley E, van der Kouwe A, Gollub R, Dale A. Reliability in multi-site structural MRI studies: effects of gradient non-linearity correction on phantom and human data. Neuroimage. 2006; 30(2):436–443. [PubMed: 16300968]

Kanwisher N, McDermott J, Chun MM. The fusiform face area: a module in human extrastriate cortex specialized for face perception. J Neurosci. 1997; 17:4302–4311. [PubMed: 9151747]

Kenet T, Bibitchkov D, Tsodyks M, Grinvald A, Arieli A. Spontaneously emerging cortical representations of visual attributes. Nature. 2003; 425:954–956. [PubMed: 14586468]

Khan S, Gramfort A, Shetty NR, Kitzbichler MG, Ganesan S, Moran JM, et al. Local and long-range functional connectivity is reduced in concert in autism spectrum disorders. Proc. Natl. Acad. Sci. U.S.A. 2013; 110:3107–3112. [PubMed: 23319621]

Kim YJ, Verghese P. The selectivity of task-dependent attention varies with surrounding context. J Neurosci. 2012; 32:12180–12191. [PubMed: 22933800]

Kolster H, Peeters R, Orban GA. The retinotopic organization of the human middle temporal area MT/V5 and its cortical neighbors. The Journal of Neuroscience. 2010; 30(29):9801–9820. [PubMed: 20660263]

Kourtzi Z, Kanwisher N. Cortical regions involved in perceiving object shape. J Neurosci. 2002; 20:3310–3318. [PubMed: 10777794]

Lampl I, Reichova I, Ferster D. Synchronous membrane potential fluctuations in neurons of the cat visual cortex. Neuron. 1999; 22:361–374. [PubMed: 10069341]

Larsson J, Heeger DJ. Two retinotopic visual areas in human lateral occipital cortex. J Neurosci. 2006; 26:13128–13142. [PubMed: 17182764]

Lin F-H, Belliveau JW, Dale AM, Hämäläinen MS. Distributed current estimates using cortical orientation constraints. Hum. Brain Mapp. 2006; 27:1–13. [PubMed: 16082624]

Litvak V, Mattout J, Kiebel S, Phillips C, Henson R, Kilner J, Barnes G, Oostenveld R, Daunizeau J, Flandin G, Penny W, Friston K. EEG and MEG data analysis in SPM8. Comput Intell Neurosci. 2011:852961. [PubMed: 21437221]

Liu Z, He B. fMRI-EEG integrated cortical source imaging by use of time-variant spatial constraints. Neuroimage. 2008; 39(3):1198–1214. [PubMed: 18036833]

Logothetis NK. What we can do and what we cannot do with fMRI. Nature. 2008; 12:869–878. [PubMed: 18548064]

Mattout J, Phillips C, Penny WD, Rugg MD, Friston KJ. MEG source localization under multiple constraints: An extended Bayesian framework. Neuroimage. 2006; 30:753–767. [PubMed: 16368248]

Neri P, Bridge H, Heeger DJ. Stereoscopic processing of absolute and relative disparity in human visual cortex. Journal of Neurophysiology. 2004; 92(3):1880–1891. [PubMed: 15331652]

Oostenveld R, Fries P, Maris E, Schoffelen JM. FieldTrip: open source software for advanced analysis of MEG, EEG, and invasive electrophysiological data. Comput Intell Neurosci. 2011:156869. [PubMed: 21253357]

Ou W, Nummenmaa A, Ahveninen J, Belliveau JW, Hämäläinen MS, Golland P. Multimodal functional imaging using fMRI-informed regional EEG/MEG. Neuroimage. 2010; 52:97–108. [PubMed: 20211266]

Park HD, Correia S, Ducorps A, Tallon-Baudry C. Spontaneous fluctuations in neural responses to heartbeats predict visual detection. Nature neuroscience. 2014; 17(4):612–618.

Pitzalis S, Strappini F, De Gasperis M, Bultrini A, Di Russo F. Spatio-temporal brain mapping of motion-onset VEPs combined with fMRI and retinotopic maps. PLoS ONE. 2012; 7:e35771. [PubMed: 22558222]

Pitzalis S, Sdoia S, Bultrini A, Committeri G, Di Russo F, et al. Selectivity to Translational Egomotion in Human Brain Motion Areas. PLoS ONE. 2013; 8(4):e60241. 2013. [PubMed: 23577096]

Reeves SJ. Optimal space-varying regularization in iterative image restoration. IEEE Trans Image Process. 1994; 3:319–324. [PubMed: 18291932]

Sato M, Yoshioka T, Kajihara S, Toyama K, Goda N, Doya K, Kawato M. Hierarchical Bayesian estimation for MEG inverse problem. Neuroimage. 2004; 23:806–826. [PubMed: 15528082]

Schmidt DM, George JS, Wood CC. Bayesian inference applied to the electromagnetic inverse problem. Hum Brain Mapp. 1999; 7:195–212. [PubMed: 10194619]

Shiozaki HM, Tanabe S, Doi T, Fujita I. Neural activity in cortical area V4 underlies fine disparity discrimination. The Journal of Neuroscience. 2012; 32(11):3830–3841. [PubMed: 22423103]

Slotnick SD, Klein SA, Carney T, Sutter E, Dastmalchi S. Using multi-stimulus VEP source localization to obtain a retinotopic map of human primary visual cortex. Clinical Neurophysiology. 1999; 110(10):1793–1800. [PubMed: 10574294]

Silver MA, Ress D, Heeger DJ. Topographic maps of visual spatial attention in human parietal cortex. J Neurophysiol. 2005; 94:1358–1371. [PubMed: 15817643]

Silver MA, Kastner S. Topographic maps in human frontal and parietal cortex. Trends Cogn Sci. 2009; 13:488–495. [PubMed: 19758835]

Smith SM. Fast robust automated brain extraction. Hum Brain Mapp. 2002; 17:143–155. [PubMed: 12391568]

Smith SM, Jenkinson M, Woolrich MW, Beckmann CF, Behrens TE, Johansen-Berg H, et al. Advances in functional and structural MR image analysis and implementation as FSL. Neuroimage. 2004; 23(Suppl 1):S208–S219. [PubMed: 15501092]

Swisher JD, Halko MA, Merabet LB, McMains SA, Somers DC. Visual topography of human intraparietal sulcus. J Neurosci. 2007; 27:5326–5337. [PubMed: 17507555]

Tadel F, Baillet S, Mosher JC, Pantazis D, Leahy RM. Brainstorm: A User-Friendly Application for MEG/EEG Analysis. Computational Intelligence and Neuroscience. 2011:1–13. [PubMed: 21837235]

Tsai JJ, Wade AR, Norcia AM. Dynamics of normalization underlying masking in human visual cortex. J Neurosci. 2012; 32:2783–2789. [PubMed: 22357861]

Tyler CW, Likova LT, Kontsevich LL, Wade AR. The specificity of cortical region KO to depth structure. NeuroImage. 2006; 30:228–238. [PubMed: 16356738]

Uutela K, Hamalainen M, Somersalo E. Visualization of magnetoencephalographic data using minimum current estimates. Neuroimage. 1999; 10:173–180. [PubMed: 10417249]

Vanni S, Warnking J, Dojat M, Delon-Martin C, Bullier J, Segebarth C. Sequence of pattern onset responses in the human visual areas: an fmri constrained vep source analysis. Neuroimage. 2004; 21(3):801–817. [PubMed: 15006647]

Verghese P, Kim YJ, Wade AR. Attention selects informative neural populations in human V1. J Neurosci. 2012; 32(46):16379–16390. [PubMed: 23152620]

Wade AR, Brewer AA, Rieger JW, Wandell BA. Functional measurements of human ventral occipital cortex: Retinotopy and colour. Philos Trans R Soc Lond B Biol Sci. 2002; 357:963–973. [PubMed: 12217168]

Wall MB, Smith AT. The Representation of Egomotion in the Human Brain. Curr Biol. 2008; 18:191–194. [PubMed: 18221876]

Wandell BA, Dumoulin SO, Brewer AA. Visual field maps in human cortex. Neuron. 2007; 56:366–383. [PubMed: 17964252]

Wipf DP, Nagarajan S. A Unified Bayesian Framework for MEG/EEG Source Imaging. Neuroimage. 2009; 44:947–966. [PubMed: 18602278]

Wolters CH, Anwander A, Tricoche X, Weinstein D, Koch MA, MacLeod RS. Influence of tissue conductivity anisotropy on EEG/MEG field and return current computation in a realistic head model: a simulation and visualization study using high-resolution finite element modeling. Neuroimage. 2006; 30:813–826. [PubMed: 16364662]

Yeatman JD, Dougherty RF, Myall NJ, Wandell BA, Feldman HM. Tract profiles of white matter properties: automating fiber-tract quantification. PLoS One. 2012; 7:e49790. [PubMed: 23166771]

Yoshioka T, Toyama K, Kawato M, Yamashita O, Nishina S, Yamagishi N, Sato M. Evaluation of hierarchical Bayesian method through retinotopic brain activities from fMRI and MEG signals. Neuroimage. 2008; 42:1397–1413. [PubMed: 18620066]
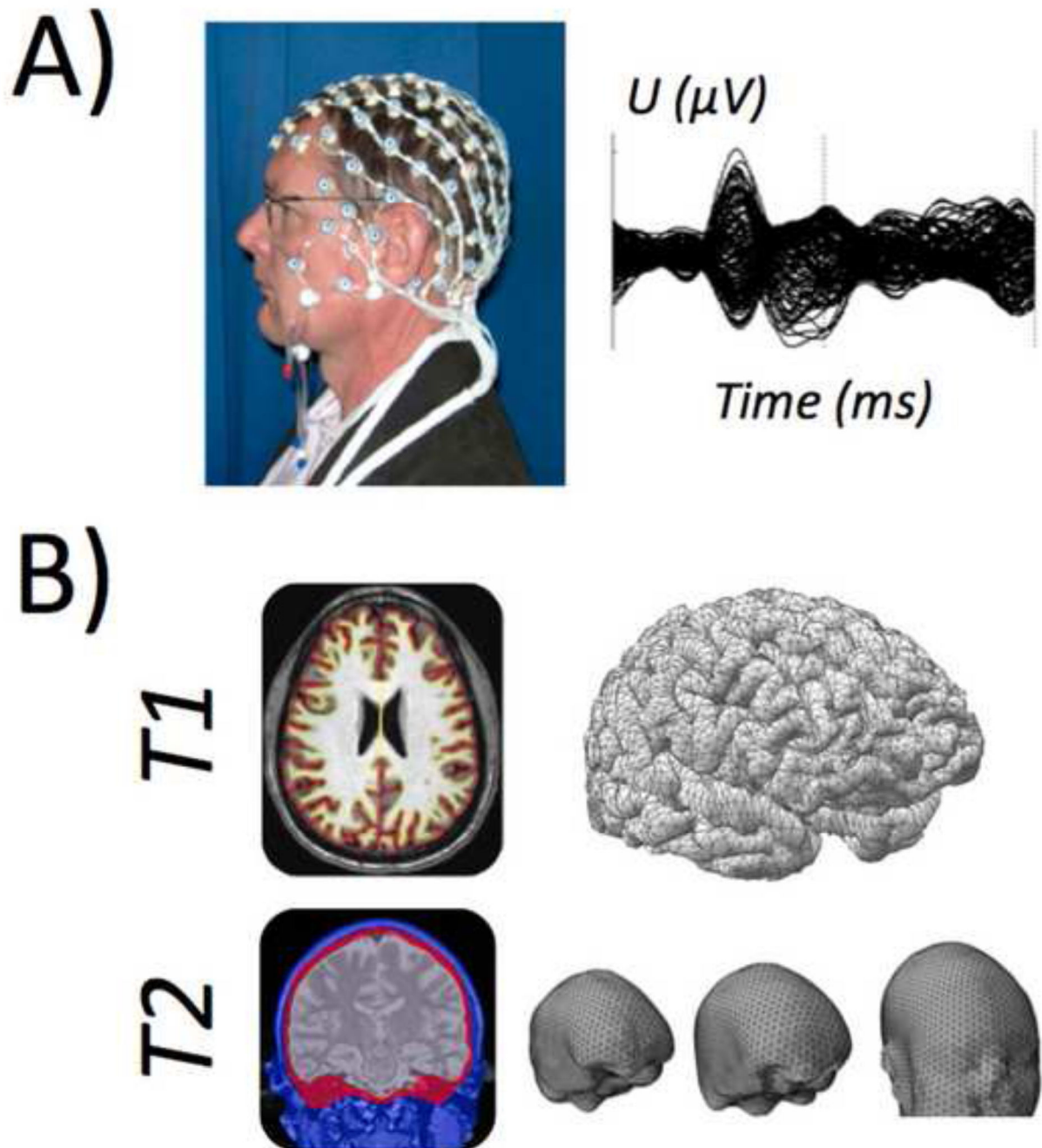
Figure 1.
Forward modeling of the EEG currents. A) EEG measurements using a high-density net (EGI system with 128 electrodes). B) Forward modeling. The source space is obtained from the segmentation of a T1 scan and is given by the 'midgray' surface. This surface is defined half-way between the white matter/gray matter (in yellow) and the gray matter/CSF (in red) boundaries (top panel). From a T2 scan (the skull is colored in red and the skin in blue), the CSF/skull, skull/skin and skin/air interfaces are extracted (bottom panel). These boundaries are used to model the linear link between each source activity and each recording.
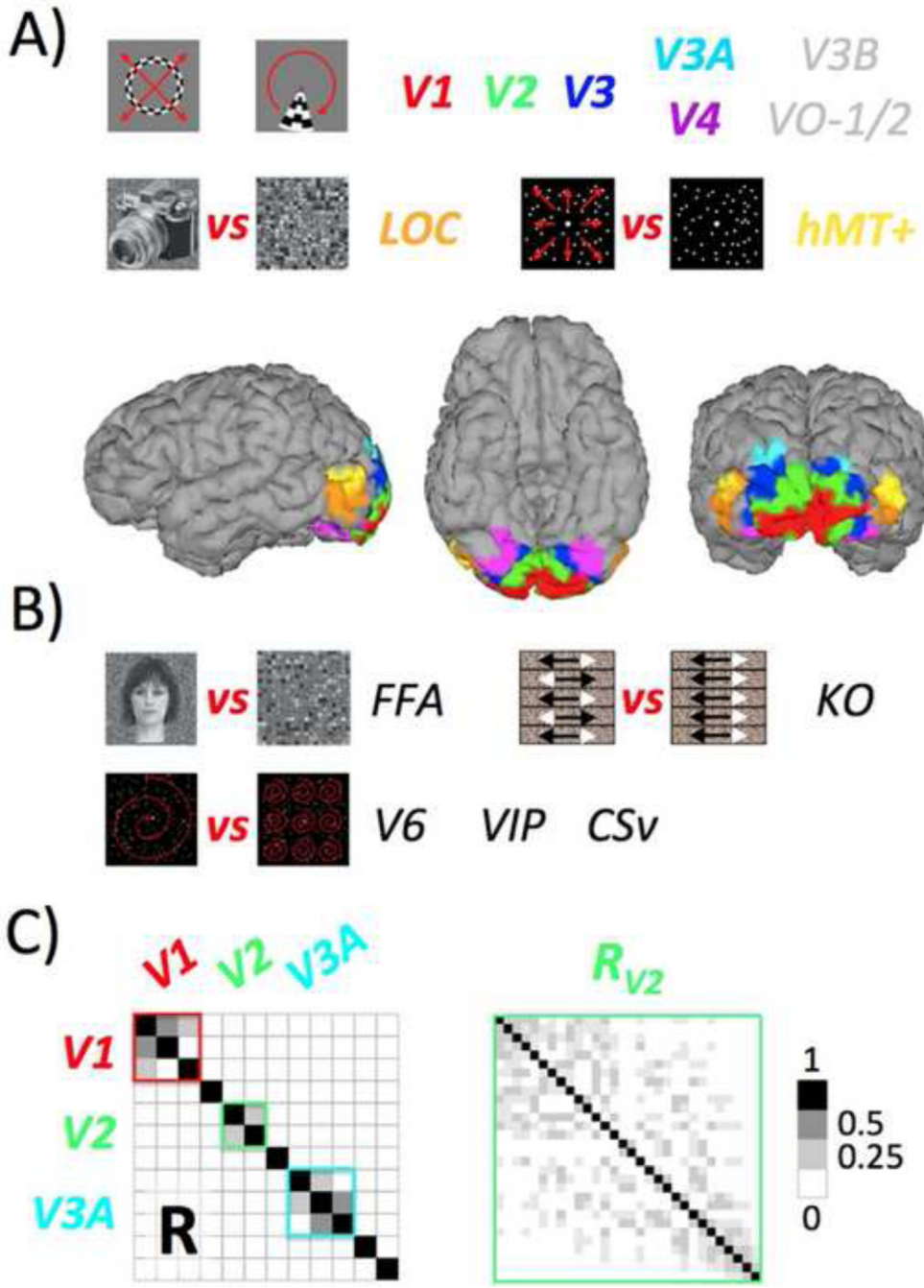
Figure 2.
fMRI localizers of the visual areas and their use in source imaging. A) Using classical retinotopic stimuli (see first row), it is possible to define areas V1, V2, V3, V4, V3A (and eventually other higher-level visual areas like e.g. V3B, VO1 or VO2) on each individual subject. The lateral occipital complex (LOC) is defined by contrasting objects with scrambled objects (second row, left). Area hMT+ is defined by contrasting coherent motion with incoherent motion (second row, right). These seven ROIs are shown on lateral, back and ventral views on a typical subject. B) Several other visual ROIs can be defined using

fMRI, e.g. the fusiform face area (FFA) that responds more to faces than to scrambled faces. Area KO responds more to depth structure stimuli. Areas V6, VIP and CSv respond more to ego-motion compatible optic flow. C) Once the functional ROIs are defined, they can be used to inform the EEG/MEG inverse problem. The sub-parts of the correlation matrix **R** that correspond to each functional area are modified. Each source within a given ROI is strongly correlated to the sources within its first and second order neighborhood that belong to the same ROI (left column). Illustration of the applied modification on the sub-part of **R** that correspond to area V2 (right column).
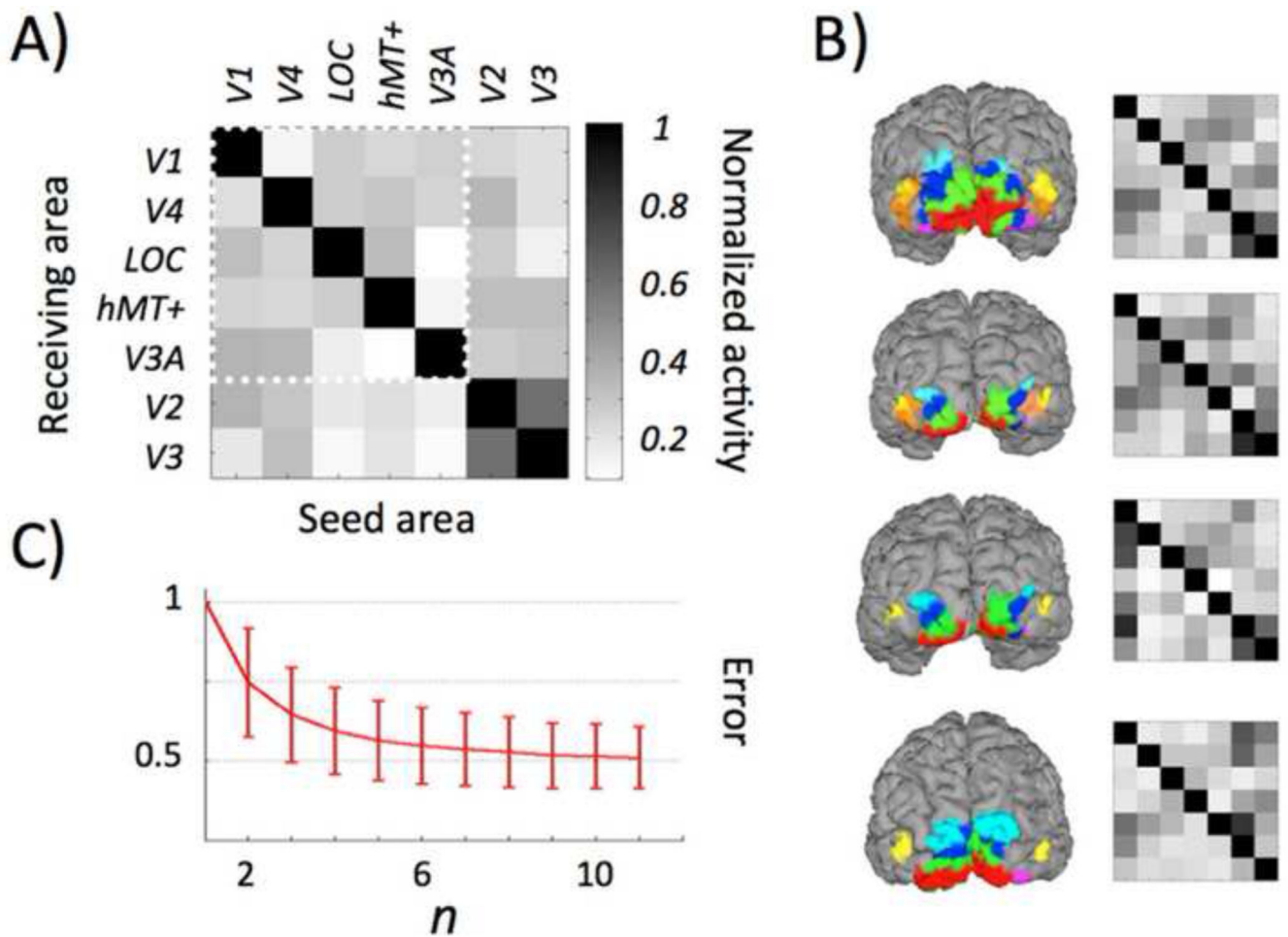
Figure 3.
Cross-talk matrix for group-level studies in EEG. A) Average cross-talk matrix for a group of eleven subjects. The cross-talk is diminished compared to that obtained at the individual level. B) Localization of area V1, V2, V3, V3A, V3, LOC and hMT+ in four subjects (see figure 2 for the colour code). The large inter-subject variability leads to very different cross-talk matrices. C) Cross-talk error as a function of the subject number. These cross-talk matrices can also be computed for group-level studies in MEG using the same approach. Tables with cross-talk values are provided in the supplements.
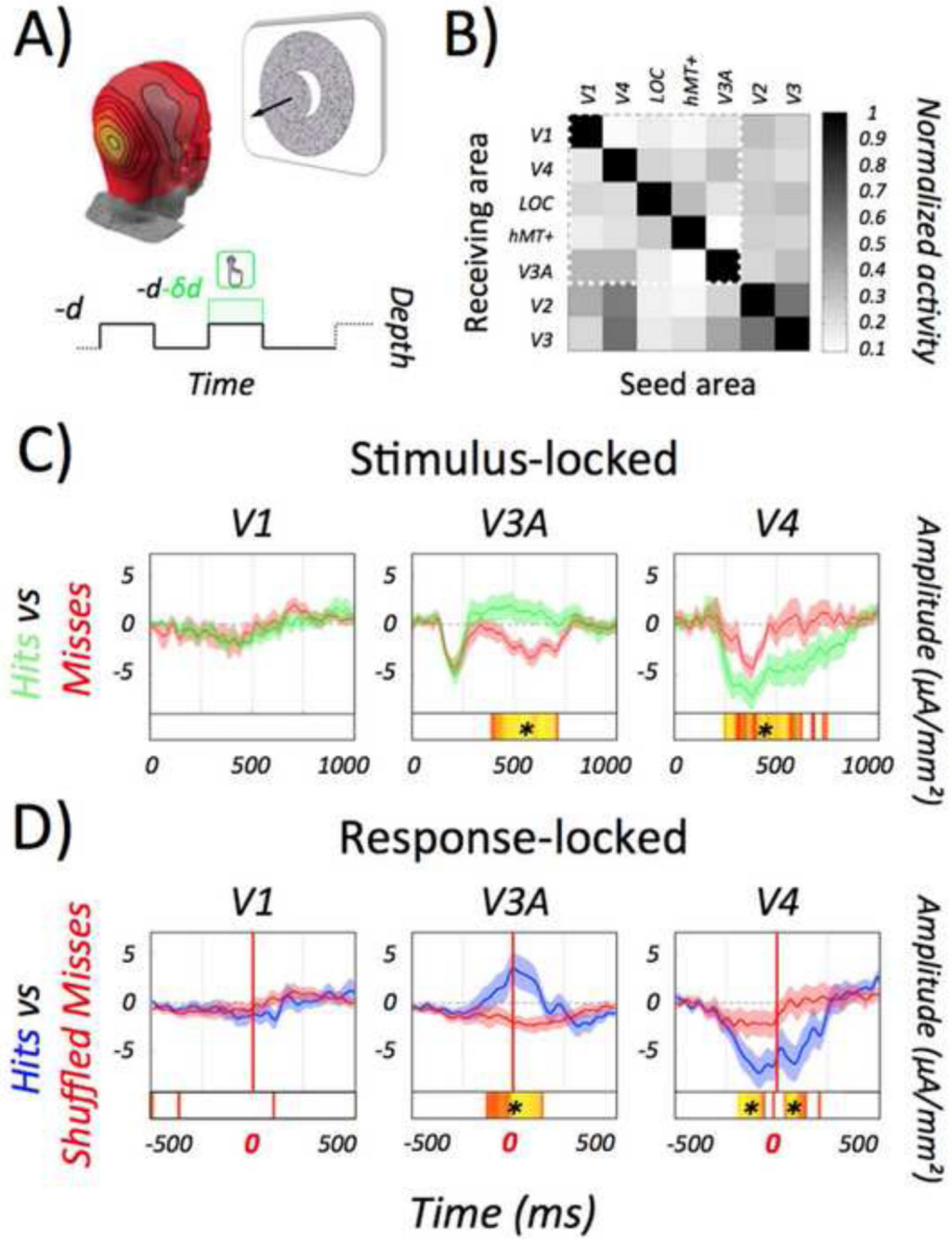
Figure 4.
Example of ROI-based analysis for the brain responses recorded in EEG during a discrimination task. A) A disparity-defined disc moved at 1Hz between the fixation plan (0 arcmin) and 5 arcmin. 30% of the time, the disparity increments was (5 + δd) arcmin and the subjects had to detect the event and to press the button (n = 11 subjects). B) Cross-talk matrix corresponding to this study (see figure 3 for the details of the legend). C) Comparison between Hits (green) and Misses (red) (stimulus-locked) in 3 representative ROIs. D)

Comparison between the response-locked data (blue) and a surrogate dataset computed from the Misses (red) in the 3 same ROIs. Figure adapted from Cottereau et al. (2014b).